Nanowire Growth

DOI: 10.1002/anie.200705142

# The Use of Single-Source Precursors for the Solution–Liquid–Solid Growth of Metal Sulfide Semiconductor Nanowires**

*Jianwei Sun and William E. Buhro**

Herein we describe the syntheses of high-quality PbS and CdS nanowires by the solution–liquid–solid (SLS) mechanism from single-source precursors. The SLS synthesis of nanowires offers several advantages over other methods, including purposeful control of nanowire mean diameters, narrow diameter distributions, small diameters in the quantum-confinement regime, control of surface passivation, nanowire solubility, and ease of implementation.[1] However, although SLS growth has been applied to a wide range of II–VI,[2] III–V,[3] and IV–VI[4] nanowire compositions, the method is not yet generally applicable, as each new composition requires extensive trial-and-error experimentation to identify appropriate precursors and reaction conditions. Our prior work has employed separate metallic-element and nonmetallic-element precursors to synthesize high-quality, compound–semiconductor nanowires.[2a,d,3d,g] Finding dual precursors with appropriately balanced reactivities has often been a primary origin of the extensive empirical experimentation required to develop a given, successful SLS nanowire synthesis. In several cases, such as for metal–sulfide semiconductors, the dual-precursor SLS approach has failed to produce highly crystalline, diameter-controlled nanowires (see Figure S1 in the Supporting Information).

We now report that the use of single-source precursors, in which the metallic and nonmetallic semiconductor constituents are combined in a single molecule, solves the reactivity-balance problem, resulting in the successful SLS growth of PbS and CdS nanowires. Therefore, the single-source approach has the potential to greatly extend the generality of the SLS method for semiconductor–nanowire synthesis. As single-source precursors have been extensively developed for use in the MOCVD growth of thin films,[5] suitable precursors for the SLS growth of many new nanowire compositions are likely already available.

Semiconductor nanowires have drawn increasing interest for their potential applications in electronic and photonic devices[6] such as field-effect transistors, light-emitting diodes, logic gates, lasers, waveguides, and solar cells. Multiple-exciton generation was recently discovered in nanocrystals of PbS and PbSe.[7] Specifically, up to four excitons (quantum yield up to 430%) were produced by absorption of a single photon in PbS nanocrystals.[7a] Although the ultrafast non-radiative Auger recombination of multiexcitons prevents the carriers from being harvested so far, this obstacle may be overcome by using elongated nanostructures, such as nanorods and nanowires.[8] If the rate of Auger recombination is significantly slower in 1D nanostructures, the efficiency of photovoltaic energy conversion might be greatly enhanced. Additionally, PbS has a relatively large exciton Bohr radius of 20 nm,[9] which makes it one of the ideal candidates for investigating quantum-confinement effects in relatively large nanostructures. The high quality of the PbS nanowires reported here enabled observation of discrete excitonic nanowire absorptions in the near infrared (NIR), allowing quantitative evaluation of the quantum confinement. The similar growth of high-quality CdS nanowires supports the generality of the single-source SLS approach.

Efforts have been made to grow PbS and CdS nanowires using the hard-template approach,[10] CVD and related approaches,[11] the solvothermal method,[12] the nanoparticle-induced anisotropic growth,[13] and surfactant-directed 1D growth.[14] However, for all of these synthetic strategies control over mean diameters and diameter distributions was limited.

Our synthetic strategy is outlined in Scheme 1. The PbS and CdS nanowires were grown by the conventional SLS mechanism,[1] except that the elements of the semiconductor phases were derived from the thermal decomposition of the single-source diethyldithiocarbamate precursors [Pb($S_2CNEt_2$)$_2$] and [Cd($S_2CNEt_2$)$_2$], respectively. These precursors have been previously used for the MOCVD growth of PbS and CdS thin films,[15] the vapor–liquid–solid (VLS) growth of CdS nanowires,[16] and the solution-based growth of PbS[17] and CdS[18] nanostructures. Bismuth nanoparticles were used to catalyze SLS growth, as we have found them

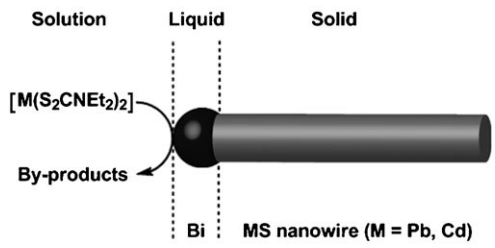


***Scheme 1.*** Solution–liquid–solid (SLS) growth of metal sulfide nanowires catalyzed by Bi nanoparticles by using [M($S_2CNEt_2$)$_2$] (M = Pb, Cd) single-source precursors.

[*] J. Sun, Prof. W. E. Buhro
Department of Chemistry and Center for Materials Innovation
Washington University
1 Brookings Drive, St. Louis, MO 63130 (USA)
Fax: (+1) 314-935-4481
E-mail: buhro@wustl.edu

[**] We thank the National Science Foundation (grant no. CHE-0518427) for support of this work, and Richard A. Loomis and John G. Glennon for assistance with NIR spectroscopy.

Supporting information for this article is available on the WWW under http://www.angewandte.org or from the author.

to be the most generally useful catalysts.[1] The minimum, controlled nanowire diameters that can typically be achieved from Bi catalysts is approximately 5 nm, because the small Bi nanoparticles ($d < 5$ nm) required to produce smaller nanowire diameters are very unstable with respect to agglomeration.

In a typical synthesis of PbS nanowires, $[Pb(S_2CNEt_2)_2]$ was first dissolved in phenyl ether with warming, and combined with a tri-*n*-octylphosphine (TOP) solution of Bi catalyst nanoparticles. The mixture was then rapidly injected into a pre-heated tri-*n*-octylphosphine oxide (TOPO) solvent or TOPO/TOP mixed solvent at a desired temperature (in the range of 210–300 °C), held at this temperature for 5 min, and allowed to cool.

Representative TEM images of the PbS nanowires shown in Figure 1 indicate that the diameters were varied over the range of 9–31 nm. The nanowires exhibited uniform diameters along their lengths, and the standard deviation in the diameter distributions was less than 30% of the mean diameter (see Figure S2 in the Supporting Information).

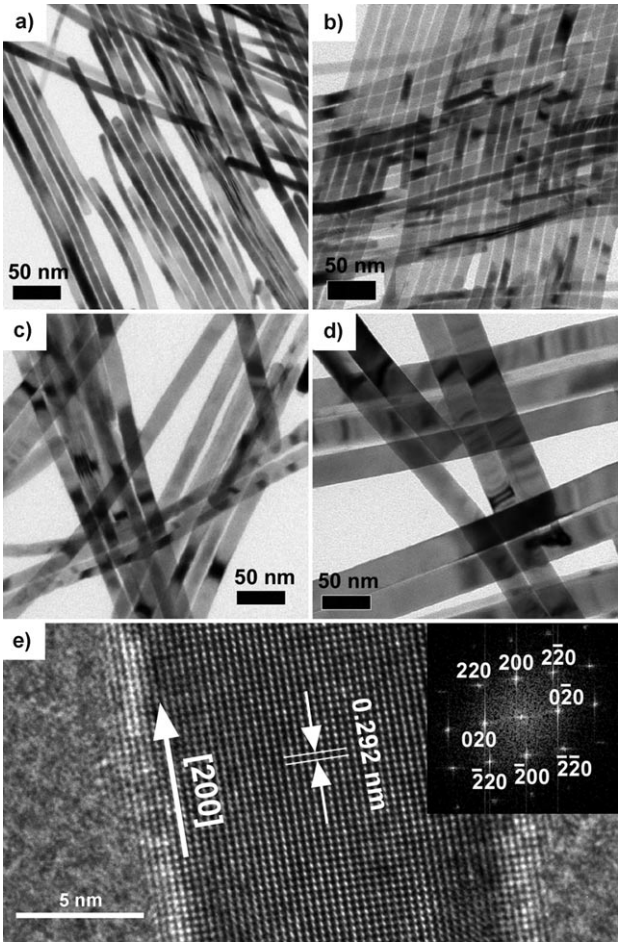


***Figure 1.*** Representative TEM images of PbS nanowires of various diameters (*d*). a) $d = (8.7 \pm 2.4)$ nm (±28%), b) $d = (11.2 \pm 2.3)$ nm (±21%), c) $d = (16.1 \pm 2.9)$ nm (±18%), and d) $d = (31.2 \pm 3.9)$ nm (±13%). e) A lattice-resolved HRTEM image of a 15 nm diameter PbS nanowire. The inset shows the indexed fast-Fourier-transform (FFT) pattern of the image, indicating that the nanowire grows along the [200] direction.

The lengths of the nanowires prepared in TOPO solvent were typically several micrometers (see Figure S3 in the Supporting Information). However, use of the TOPO/TOP mixed solvent enabled controlled growth of shorter nanowires (see Figure S4 in the Supporting Information), with mean lengths dependent on the TOPO/TOP ratio. Lower TOPO/TOP ratios produced shorter nanowires. Long nanowires tended to form bundles, likely as a result of strong Van der Waals attractions between the nanowires.[19] Catalyst nanoparticles were observed at one end of the wires (see Figure S5 in the Supporting Information), confirming the SLS growth mechanism.[1] Control experiments conducted without Bi-catalyst nanoparticles produced no nanowire growth (see Figure S6 in the Supporting Information).

The mean nanowire diameters were controlled by varying the reaction temperature, and by using an additional surfactant, *n*-tetradecylphosphonic acid (TDPA) (see Table S1 in the Supporting Information). Larger nanowire diameters were favored at higher reaction temperatures using Bi nanoparticles of a given diameter. Thus, 10.3 nm Bi nanoparticles produced 11.0 nm and 13.3 nm nanowire diameters at 232 and 277 °C, respectively. Reactions carried out at about 210 °C were unsuccessful. The use of a small amount of TDPA in the synthesis resulted in 8.7 nm PbS nanowires. However, the amount of TDPA was critical; TDPA/Cd ratios larger than 1 produced short wires, cubes, and irregularly shaped particles. Another commonly used naowire surfactant, *n*-hexadecylamine (HDA), was found to be synthetically detrimental in this system (see Figure S7 in the Supporting Information). The naowire diameters were typically *larger* than the initial diameters of the Bi nanoparticles, especially for smaller-diameter Bi nanoparticles. The *largest* nanowires (31 nm diameter) were obtained from the *smallest* (4.3 nm) Bi nanoparticles. A minority population of 8.9 nm nanowires was also produced under these conditions. The results indicated that the nanowires grew from larger Bi nanoparticles formed by nanoparticle agglomeration. Because the smallest Bi nanoparticles exhibit the strongest agglomeration tendencies, the best nanowire diameter control was achieved with the larger-diameter catalyst nanoparticles.

The expected rock-salt structure of the PbS nanowires was confirmed by powder X-ray diffraction (XRD, see Figure S8 in the Supporting Information) and high-resolution transmission electron microscopy (HRTEM, Figure 1e). The single-crystalline nature of the nanowires was clearly evidenced in the HRTEM image (Figure 1e), in which the {200} lattice fringes were well resolved and exhibited the correct spacing of 0.292 nm.[20] The fast-Fourier-transform (FFT) pattern of the PbS nanowire lattice was indexed to the rock-salt structure (inset, Figure 1e), and indicated a [200] growth direction for the nanowires.

Strong quantum confinement in the PbS nanowires was confirmed by NIR absorption spectroscopy. A typical spectrum (Figure 2) of an 11.2 nm-diameter specimen clearly shows two well-resolved excitonic features. The position of the first excitonic feature was determined to be 2343 nm by background fitting and subtraction (see Figure S9 in the Supporting Information).[2a] This feature is strongly blue-shifted in comparison to the PbS bulk absorption edge at

  

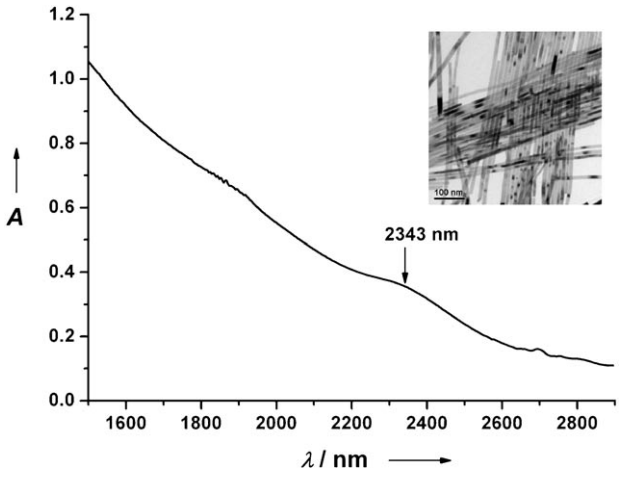


***Figure 2.*** NIR absorption spectrum of colloidal PbS nanowires with a mean diameter of 11.2 nm, dispersed in carbon tetrachloride. The first excitonic feature, centered at 2343 nm, is identified by an arrow. The inset shows a TEM image of this sample.

3024 nm, corresponding to a quantum confinement of $\Delta E_g =$ 119 meV. As expected, because the bulk exciton Bohr radius in PbS is quite large (20 nm), 11.2 nm diameter PbS nanowires are strongly confined. The photoluminescence of the PbS nanowires was not investigated.

To demonstrate the potential generality of the single-source SLS synthetic strategy, CdS nanowires were also similarly grown from $[Cd(S_2CNEt_2)_2]$. Representative TEM images (Figure 3 a–c) show that this SLS strategy afforded high-quality nanowires with smaller diameters in the range of 7–11 nm than did the VLS method using the same precursor.[16] The standard deviations in the diameter distributions of the SLS-grown nanowires were below 20% of the mean diameters (see Figure S10 in the Supporting Information), which were narrower than the distributions achieved by the VLS method. The wurtzite crystal structure of the nanowires was confirmed by XRD (see Figure S11 in the Supporting Information) and by the FFT pattern from an HRTEM image (Figure 3 d inset). The well-resolved lattice fringes perpendicular to the growth direction in the HRTEM image corresponded to a spacing of 0.330 nm, consistent with the (002) planes in hexagonal CdS.[21] The indexed FFT pattern confirmed the [002] nanowire growth direction.

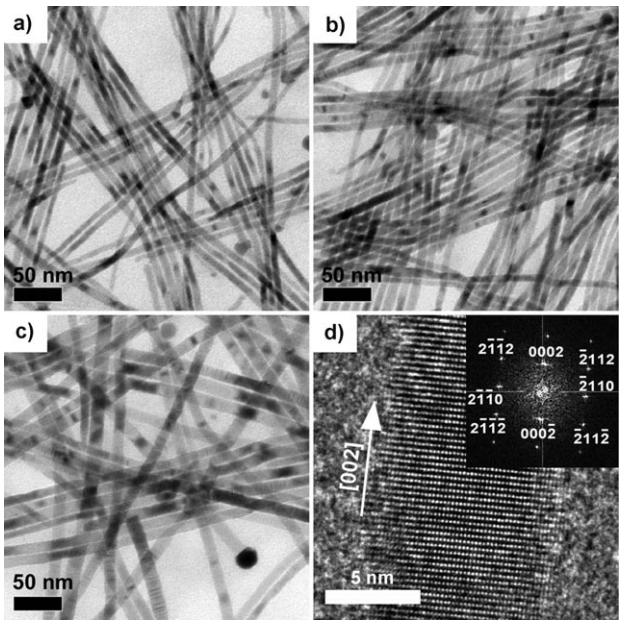


***Figure 3.*** Representative TEM images of CdS nanowires of various diameters ($d$). a) $d = (6.9 \pm 1.3)$ nm ($\pm 19\%$), b) $d = (7.8 \pm 1.2)$ nm ($\pm 15\%$), and c) $d = (11.0 \pm 1.8)$ nm ($\pm 16\%$). d) A lattice-resolved HRTEM image of a 9 nm diameter CdS nanowire. The inset shows the indexed fast-Fourier-transform (FFT) pattern of the image, indicating that the nanowire grows along the [002] direction.

In conclusion, we have demonstrated that colloidal PbS and CdS semiconductor nanowires may be grown by the SLS mechanism using single-source precursors. Excellent diameter control was achieved. The high quality of the PbS nanowires enabled us to observe well-resolved NIR excitonic absorption features, confirming strong quantum confinement. These PbS and CdS nanowires are candidates for further fundamental studies, and for potential applications in solar cells[7a] and photodetectors.[22] Moreover, the results described here strongly suggest that the single-source SLS strategy may extend to other colloidal semiconductor nanowire systems that are not easily prepared by a dual-source precursor approach.

## *Experimental Section*

Materials: Lead(II) nitrate (99.999%, Aldrich), cadmium chloride (99.995%, Strem), sodium diethyldithiocarbamate trihydrate (ACS grade, Alfa Aesar), phenyl ether (99%, Acros), tri-*n*-octylphosphine (TOP, 90%, Aldrich), tri-*n*-octylphosphine oxide (TOPO, 99%, Aldrich), and *n*-tetradecylphosphonic acid (TDPA, PolyCarbon Industries) were purchased and used as received. Technical-grade TOPO (90%, Aldrich) was vacuum distilled before use. The single-source precursors $[M(S_2CNEt_2)_2]$ (M = Cd,[23] Pb[17a]) were prepared by literature methods. The Bi-nanoparticle stock solutions were prepared as previously described.[2a] All procedures for the synthesis of nanowires were conducted under dry, $O_2$-free $N_2$(g).

Synthesis of PbS nanowires: In a typical synthesis, TOPO (90%-purity grade, 4.0 g) was loaded into a Schlenk reaction tube with a small magnetic stir bar. Separately, $[Pb(S_2CNEt_2)_2]$ (20 mg, 0.04 mmol) and phenyl ether (0.8 g) were combined in a small vial. In a separate small vial, a Bi-nanoparticle stock solution (15 mg) was combined with TOP (0.5 g). The reaction tube was then inserted in a pre-heated salt bath ($NaNO_3/KNO_3$, 46:54 by weight) at 250 °C for at least 5 min to allow the temperature to equilibrate. The Bi-nanoparticle mixture was loaded into a 2 mL syringe. The $[Pb(S_2CNEt_2)_2]$ mixture was gently heated with a heat gun until a homogeneous solution was obtained (< 1 min). This hot solution was loaded into the syringe containing the Bi nanoparticles. The contents of the syringe were rapidly injected into the pre-heated, stirred TOPO. The reaction mixture turned black within 10 s. After the reaction mixture was stirred for 5 min, the reaction tube was withdrawn from the salt bath and allowed to cool. While cooling, toluene ($\approx$5 mL) was added to prevent solidification. The conditions and results for various PbS nanowire syntheses are summarized in Table S1 in the Supporting Information.

Synthesis of CdS nanowires: In a typical synthesis, TDPA (7 mg, 0.025 mmol) and TOPO (99%-purity grade, 4.0 g) were loaded into a Schlenk reaction tube with a small magnetic stir bar. Separately, $[Cd(S_2CNEt_2)_2]$ (40 mg, 0.1 mmol) and TOP (0.8 g) were combined in

  

a small vial, into which a Bi-nanoparticle stock solution (25 mg) was added. The $[Cd(S_2CNEt_2)_2]$ slowly dissolved in the mixture to form a homogeneous solution. The reaction tube was then inserted in a preheated salt bath ($NaNO_3/KNO_3$, 46:54 by weight) at 250 °C for at least 5 min to allow the temperature to equilibrate. The contents of the vial were loaded into a 2 mL syringe, and rapidly injected into the preheated, stirred reaction tube. The reaction mixture turned a yellowish color within 10 s. After the reaction mixture was stirred for 5 min, it was withdrawn from the salt bath and allowed to cool. While cooling, toluene ($\approx$5 mL) was added to prevent solidification. The conditions and results for various CdS nanowire syntheses are summarized in Table S2 in the Supporting Information.

Isolation and characterization: The nanowires were separated from the cooled reaction mixtures by addition of methanol ($\approx$10 mL). The precipitated wires were collected by centrifugation and the supernatant was decanted. The wires were then redispersed in hexane (1 mL) and reprecipitated by addition of acetone ($\approx$10 mL), followed by centrifugation and decantation. This process was repeated 2–3 times to remove the by-products generated during the reactions. The purified wires were redispersed in toluene for TEM sample preparation. However, for the NIR study the purified wires were dried under a stream of $N_2$ to remove volatile organics, and then redispersed in carbon tetrachloride. Carbon-coated Cu TEM grids were prepared by evaporating one drop of the nanowire toluene solutions on them. TEM images were collected using a JEOL 2000 FX microscope at 200 kV. The HRTEM images were collected by using a JEOL JEM-2100F microscopy at 200 kV. The XRD pattern was obtained by using a Rigaku Dmax A vertical powder diffractometer with $Cu_{K\alpha}$ radiation ($\lambda = 1.5418$ Å). The NIR spectrum was collected by using a Perkin–Elmer Lamda 950 UV-Vis-NIR spectrometer.

Received: November 7, 2007
Published online: March 19, 2008

**Keywords:** bismuth · colloids · crystal growth · nanowires · semiconductors

[1] F. Wang, A. Dong, J. Sun, R. Tang, H. Yu, W. E. Buhro, *Inorg. Chem.* **2006**, *45*, 7511.
[2] a) H. Yu, J. Li, R. A. Loomis, P. C. Gibbons, L. W. Wang, W. E. Buhro, *J. Am. Chem. Soc.* **2003**, *125*, 16168; b) J. W. Grebinski, K. L. Hull, J. Zhang, T. H. Kosel, M. Kuno, *Chem. Mater.* **2004**, *16*, 5260; c) M. Kuno, O. Ahmad, V. Protasenko, D. Bacinello, T. H. Kosel, *Chem. Mater.* **2006**, *18*, 5722; d) A. Dong, F. Wang, T. L. Daulton, W. E. Buhro, *Nano Lett.* **2007**, *7*, 1308; e) L. Ouyang, K. N. Maher, C. L. Yu, J. McCarty, H. Park, *J. Am. Chem. Soc.* **2007**, *129*, 133; f) D. D. Fanfair, B. A. Korgel, *Chem. Mater.* **2007**, *19*, 4943.
[3] a) T. J. Trentler, K. M. Hickman, S. C. Goel, A. M. Viano, P. C. Gibbons, W. E. Buhro, *Science* **1995**, *270*, 1791; b) T. J. Trentler, S. C. Goel, K. M. Hickman, A. M. Viano, M. Y. Chiang, A. M. Beatty, P. C. Gibbons, W. E. Buhro, *J. Am. Chem. Soc.* **1997**, *119*, 2172; c) S. D. Dingman, N. P. Rath, P. D. Markowitz, P. C. Gibbons, W. E. Buhro, *Angew. Chem.* **2000**, *112*, 1530; d) H. Yu, W. E. Buhro, *Adv. Mater.* **2003**, *15*, 416; e) H. Yu, J. Li, R. A. Loomis, L.-W. Wang, W. E. Buhro, *Nat. Mater.* **2003**, *2*, 517; f) D. D. Fanfair, B. A. Korgel, *Cryst. Growth Des.* **2005**, *5*, 1971; g) F. Wang, H. Yu, J. Li, Q. Hang, D. Zemlyanov, P. C. Gibbons, L. W. Wang, D. B. Janes, W. E. Buhro, *J. Am. Chem. Soc.* **2007**, *129*, 14327.
[4] K. L. Hull, J. W. Grebinski, T. H. Kosel, M. Kuno, *Chem. Mater.* **2005**, *17*, 4416.
[5] a) A. H. Cowley, R. A. Jones, *Angew. Chem.* **1989**, *101*, 1235; *Angew. Chem. Int. Ed. Engl.* **1989**, *28*, 1208; b) P. O'Brien, R. Nomura, *J. Mater. Chem.* **1995**, *5*, 1761; c) M. Bochmann, *Chem. Vap. Deposition* **1996**, *2*, 85; d) D. A. Neumayer, J. G. Ekerdt, *Chem. Mater.* **1996**, *8*, 9; e) A. N. Gleizes, *Chem. Vap. Deposition* **2000**, *6*, 155.
[6] a) Y. Li, F. Qian, J. Xiang, C. M. Lieber, *Mater. Today* **2006**, *9*, 18; b) C. Thelander, P. Agarwal, S. Brongersma, J. Eymery, L. F. Feiner, A. Forchel, M. Scheffler, W. Riess, B. J. Ohlsson, U. Gosele, L. Samuelson, *Mater. Today* **2006**, *9*, 28; c) P. J. Pauzauskie, P. Yang, *Mater. Today* **2006**, *9*, 36; d) M. Law, L. E. Greene, J. C. Johnson, R. Saykally, P. Yang, *Nat. Mater.* **2005**, *4*, 455.
[7] a) R. D. Schaller, M. Sykora, J. M. Pietryga, V. I. Klimov, *Nano Lett.* **2006**, *6*, 424; b) R. J. Ellingson, M. C. Beard, J. C. Johnson, P. Yu, O. I. Micic, A. J. Nozik, A. Shabaev, A. L. Efros, *Nano Lett.* **2005**, *5*, 865.
[8] V. I. Klimov, *J. Phys. Chem. B* **2006**, *110*, 16827.
[9] F. W. Wise, *Acc. Chem. Res.* **2000**, *33*, 773.
[10] a) F. Gao, Q. Lu, X. Liu, Y. Yan, D. Zhao, *Nano Lett.* **2001**, *1*, 743; b) R. Thiruvengadathan, O. Regev, *Chem. Mater.* **2005**, *17*, 3281.
[11] a) M. Fardy, A. I. Hochbaum, J. Goldberger, M. M. Zhang, P. Yang, *Adv. Mater.* **2007**, *19*, 3047; b) M. J. Bierman, Y. K. A. Lau, S. Jin, *Nano Lett.* **2007**, *7*, 2907; c) J.-P. Ge, J. Wang, H.-X. Zhang, X. Wang, Q. Peng, Y.-D. Li, *Chem. Eur. J.* **2005**, *11*, 1889.
[12] K.-B. Tang, Y.-T. Qian, J.-H. Zeng, X.-G. Yang, *Adv. Mater.* **2003**, *15*, 448.
[13] K. T. Yong, Y. Sahoo, K. R. Choudhury, M. T. Swihart, J. R. Minter, P. N. Prasad, *Chem. Mater.* **2006**, *18*, 5965.
[14] a) I. Patla, S. Acharya, L. Zeiri, J. Israelachvili, S. Efrima, Y. Golan, *Nano Lett.* **2007**, *7*, 1459; b) S. Acharya, I. Patla, J. Kost, S. Efrima, Y. Golan, *J. Am. Chem. Soc.* **2006**, *128*, 9294.
[15] N. I. Fainer, M. L. Kosinova, Y. M. Rumyantsev, E. G. Salman, F. A. Kuznetsov, *Thin Solid Films* **1996**, *280*, 16.
[16] C. J. Barrelet, Y. Wu, D. C. Bell, C. M. Lieber, *J. Am. Chem. Soc.* **2003**, *125*, 11498.
[17] a) T. Trindade, P. O'Brien, X.-M. Zhang, M. Motevalli, *J. Mater. Chem.* **1997**, *7*, 1011; b) S.-M. Lee, Y.-W. Jun, S.-N. Cho, J. Cheon, *J. Am. Chem. Soc.* **2002**, *124*, 11244.
[18] a) P. Yan, Y. Xie, Y. Qian, X. Liu, *Chem. Commun.* **1999**, 1293; b) Y.-W. Jun, S.-M. Lee, N.-J. Kang, J. Cheon, *J. Am. Chem. Soc.* **2001**, *123*, 5150; c) Y. C. Zhang, G. Y. Wang, X. Y. Hu, *J. Alloys Compd.* **2007**, *437*, 47.
[19] S. Fan, M. G. Chapline, N. R. Franklin, T. W. Tombler, A. M. Cassell, H. Dai, *Science* **1999**, *283*, 512.
[20] ICDD-PDF No. 01-072-4873.
[21] ICDD-PDF No. 01-075-1545.
[22] S. A. McDonald, G. Konstantatos, S. Zhang, P. W. Cyr, E. J. D. Klem, L. Levina, E. H. Sargent, *Nat. Mater.* **2005**, *4*, 138.
[23] O. F. Z. Khan, P. O'Brien, *Polyhedron* **1991**, *10*, 325.

  